TURBOMACHINERY & PUMP SYMPOSIA | HOUSTON, TX
DECEMBER 14-16, 2021
SHORT COURSES: DECEMBER 13, 2021

Cavitation Prediction and Avoidance in Design using Semi-Empirical 1D Models with Fast 3D CFD Validation

Vlad Goldenberg
Consulting Engineer
SoftInWay Inc.
Burlington, Massachusetts, USA

Evgen Rublevskiy
Principal Engineer
SoftInWay Switzerland GmbH
Zug, Switzerland

Tishun Zhang
Consulting Engineer
SoftInWay Switzerland GmbH
Zug, Switzerland

Andrey Sherbina
Principal Engineer
SoftInWay Switzerland GmbH
Zug, Switzerland

Ben Conser
Applications Engineer
SoftInWay Inc.
Burlington, Massachusetts, USA

Vlad Goldenberg is a consulting engineer at SoftInWay in charge of leading compressor and pump R&D and consulting projects. He has over a decade of previous experience working in the power generation and refrigeration industries involved in machinery and high energy systems. He holds a Ph.D. in mechanical engineering from the University of Minnesota. Previous degrees were obtained from the University of St. Thomas and U.C. Berkeley. He is currently a licensed professional engineer in the state of Minnesota. Vlad highly enjoys downhill skiing, and always seeks new friendships on the piste, and eagerly awaits when his young son is old enough to be introduced to this wonderful winter activity.

ABSTRACT

Cavitation is a phenomenon that is of great concern to both the design and operation of pumps. The presence of cavitation – that is, the formation of vapor bubbles in the flowing fluid that subsequently collapses – can cause severe consequences from degradation of performance to damage mechanisms and even to catastrophic failure. Therefore, it is desired to predict under what conditions and design parameters cavitation occurs. Historically, the Net Positive Suction Head (NPSH) parameter and its various flavors (i.e. actual NPSH, available NPSH, required NPSH, 3% NPSH, etc.) have been used to characterize the pressure required at or near the pump inlet, to avoid the effects of cavitation. An important operational aspect of the required NPSH that is often ignored or perhaps unknown to many practitioners is that it is variable and depends on operational parameters, including rotor speed and fluid flow rate. The challenge is heightened in design, where geometry parameters also influence cavitation.

The difficulty, at least in part, with cavitation is that the physical phenomenon of cavitation is separated from the effects of cavitation that are directly observable or measurable experimentally. That is, the physical phenomenon of cavitation occurs when local static pressure in a flow field drops below the vapor pressure of the fluid. However, influencing parameters, such as the presence of nucleation sites, the spatial and temporal extent of the local low pressure zone, the path of the flow field, and the wall boundaries all contribute effects that are not fully understood. Such dependencies are contributors to, for example, the observed cavitation damage seen in pump impellers that otherwise exhibit no cavitation related performance effects. This is also apparent in the cavitation characteristic often examined to evaluate the cavitation performance and required NPSH. The cavitation characteristic, a plot of the NPSH on the Abscissa and the total discharge head (TDH) on the ordinate, has historically been used to characterize cavitation because TDH can be directly measured experimentally. However, the location where cavitation damage can occur is usually several times the NPSH where measurable reduction in TDH occurs.

In this work, the theoretical underpinnings that cause the physical phenomenon of cavitation are examined and used to develop a modern computational method using CFD of evaluating the cavitation characteristic from both a classical measurement perspective where TDH is affected, as well as the phenomenological perspective where vapor zone formation is tracked. This work shows that steady state RANS CFD, when combined with use of the Rayleigh-Plesset cavitation model, is able to effectively predict both onset of cavitation and the drop in TDH with computational expense that is order of magnitude less costly than the transient CFD methods that have previously been deployed on such problems

Furthermore, it is shown in this work that effective design to avoid cavitation by accurate prediction of the semi-empirical required NPSH method first developed by Lomakin can be used directly in the design process. The implemented design process uses low-order and low computational cost numerical algorithms to solve the fluid flow and categorize many design candidates by parameters of interest, including the required NPSH.

This work also enhances the semi-empirical Lomakin method for predicting cavitation with a modified correction for accounting for flow conditions of non-zero incidence. Under severe non-zero incidence conditions, there may exist one or more zones of local flow separation and low pressure region, or under mild incidence the flow may be attached but also is associated with local pressure in the flow field falling below the saturated vapor pressure, and this situation frequently occurs at most operating points away from the design condition. An attached sheet of cavitation bubbles can travel along the blade surface under certain conditions. It is shown that an empirically derived coefficient using the steady state CFD methodology previously discussed informs a fast reduced-order model that is accurate and can be utilized for quickly generating the NPSH maps of various potential design candidates and is therefore invaluable in pump design work.

INTRODUCTION

Pump cavitation starts when the local suction static pressure near the inlet of a pump decreases below the local vapor pressure of the working fluid. This causes the local working fluid to vaporize and can cause the formation of bubbles within the fluid flow. These bubbles will then implode when they flow into a local high-pressure region further along the flow field. This bubble implosion can cause noise, vibration, and damage to the machine surface. The accumulated damage from these implosions can lead to reduced performance and machine lifetime with an increase in noise, pressure pulsations, torque fluctuations, and vibrations (Schiavello and Visser, 2009).

Because of this degradation of pump performance, it is desired to predict the operating conditions for which a given pump will cavitate. To aid in this prediction, the Net Positive Suction Head (NPSH) parameter is typically used. To keep the fluid from vaporizing, the available NPSH (NPSHa) describes how much greater the local static pressure at the inlet of the pump is relative to the local vapor pressure of the fluid at the pump inlet. These parameters are typically analyzed at steady-state operating conditions, however NPSH transients can occur when pumps are transitioning between operating states (Czyszcewski, 2021).

When the local inlet static pressure decreases below the local vapor pressure, bubbles may start to form, and cavitation may start to occur. The local static pressure at which this occurs is a function of the local fluid temperature, and the corresponding local vapor pressure. The minimum required suction head needed to prevent this operating condition from occurring or to prevent certain of its effects from being felt (to be defined further later) is the required NPSH (NPSHr). Since NPSHr is related to when the local inlet static pressure is minimized, it is also related to when the dynamic pressure of the inlet flow (and the corresponding inlet fluid velocity) is maximized. As NPSHr is related to the fluid velocity, operating parameters such as the rotor speed and fluid flow rate will cause the value of NPSHr to vary for a given pump geometry.

While the onset of the physical phenomenon of cavitation may occur at a particular inlet pressure, a drop in performance due to cavitation is not observed until the inlet pressure is dropped even lower. Although the parameter characterizing the amount by which the head rise capability drops may vary between manufacturers, a standard parameter is 3% NPSH (NPSH3), which describes the inlet pressure corresponding with a 3% drop in the head rise capability of the pump. Each operating point (a particular rotor speed and fluid flow rate) will have a unique NPSH3 value. Understanding how NPSH3 varies with flow rate for a machine and its relation to the inlet flow conditions (and the NPSHa) will help a designer understand the allowable operating range for which a given machine will not experience harmful effects of cavitation. The relation between NPSHa and NPSHr, either the difference and/or the ratio of these values, are commonly used to predict cavitation (Schiavello and Visser, 2009).

A very useful and common tool to evaluate and understand cavitation performance of any particular machine is the cavitation characteristic. A conceptual sketch of a characteristic is shown in Figure 1. Traditionally, such a characteristic was established experimentally by placing the machine in a test loop whereby the suction conditions could be throttled or the temperature modified in progressive tests while monitoring pump performance parameters. Thereby, each test condition would result in progressively decreasing available suction head and TDH can be plotted for each test condition until drastic drop off was achieved.

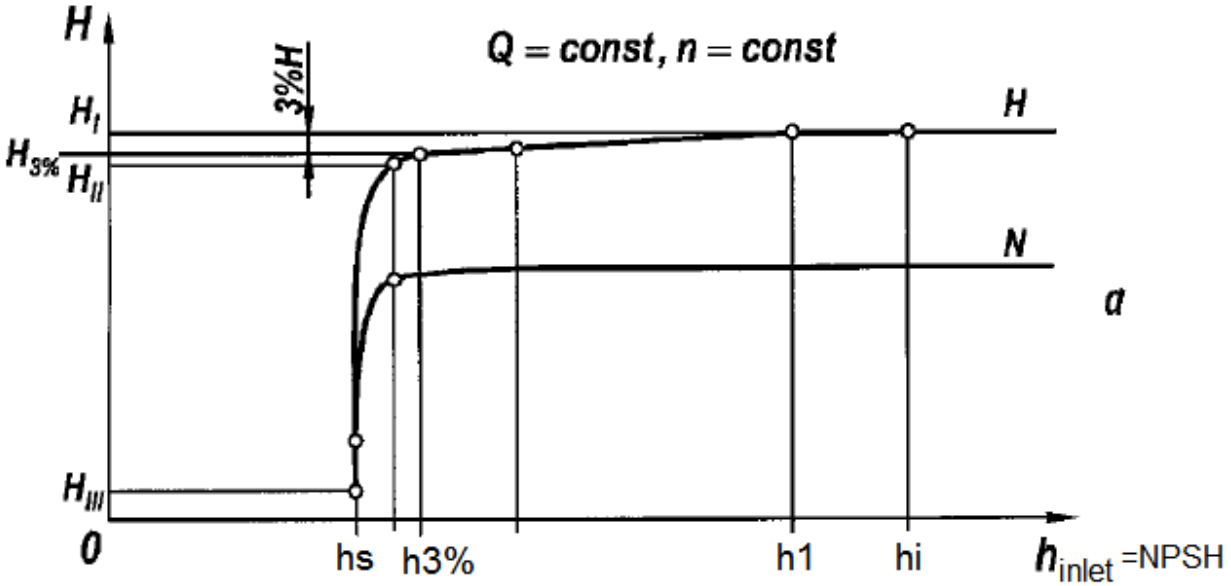

Figure 1 - Conceptual sketch of a cavitation characteristic showing h_i (inception), h_1 (first head drop appearance), h_3 (NPSH3), and h_s (supercavitation breakdown)

With modern computation and simulation capabilities, such experiments can be done virtually using a full geometry model of the candidate machine and modern CFD codes. The methods for doing so will be described further in this work. However, it will be noted that these methods are well tried and tested. Sample research that achieved also good results with these methods are (Mejri et. al., 2005), (Li, 2014), and (Pei et. al., 2019). Pei, Osman, Wang, Appiah, Yin, and Deng (2019) particularly pioneered an enhanced method for deriving the characteristic curves using CFD that is based on the same approach as is used in this work. Although their method is not implemented here, it is potentially very useful to reduce resource constraints in future work.

A very important aspect to emphasize is that cavitation is the physical phenomenon of bubble formation through local vaporization of fluid at some point in the flow path, potentially followed by a collapse mechanism downstream in the flow path. The actual phenomenon is what we know physically occurs due to the physics of the situation. The effects of cavitation are diverse, and it is typically these effects that pump designers and users seek to avoid. The effects can be vibration, damage, performance degradation, or other effects. As was expounded in detail by Schiavello and Visser (2009), damage mechanisms from cavitation may start to present themselves quite near the suction conditions of cavitation inception, yet the acute performance impact is not apparent until perhaps a long time of operation where the damage has already occurred. In fact, the most damaging zone is often between the inception point and where TDH degrades by 3% (Schiavello and Visser, 2009). This is the painful situation that pump practitioners have to contend with – that often is difficult to predict because non-acute effects are actually difficult to measure.

Cavitation is a transient phenomenon, as the growth and size of the bubbles depends on both the liquid thermodynamic conditions and time since nucleation. A common method for modeling the bubble growth dynamics is the Rayleigh-Plesset equation, as shown by Brennen (1995). This model uses a mass transfer approach to describe the bubble dynamics which includes the influence of bubble growth acceleration, viscous effects, and surface tension effects. Details of this model will be discussed later. Other models, such as the Schnerr-Sauer cavitation model (shown below), is based on a reduced Rayleigh-Plesset equation, where the influence of bubble growth acceleration, viscous effects, and surface tension effects are neglected. Additional models for fluid with extensive cavitation and large density ratios have also been developed (Bakir *et al.*, 2004).

Several analysis approaches have also been developed to find relations and functions in cavitation prediction to either aid the predictive capability of a given cavitation model or to speed up the computation time required by a particular cavitation model. These include using a VOF technique with a truncated Rayleigh-Plesset model (Mejri *et al*. 2005), predicting NPSHr using a function relating flow rate and the cavitating VOF (Marini *et al.*, 2011), exploring the relationship between pump head and integrated vapor-liquid volume ratio (Li, 2014), as well as developing a new methodology of setting the outlet static pressure when determining NPSHr (Pei *et al*., 2019).

While using these cavitation models in 3D CFD may give us physically accurate results, the nature of the CFD approach makes attaining these results very time consuming and computationally expensive. When performing a quick iterative design approach, especially earlier in the design process, the time it takes to attain the cavitation performance results from CFD is often too long for practical design iteration. The 1D cavitation methodology shown in this work takes much less time and computational resources, while still providing reasonably accurate results when compared against those of 3D CFD and is especially useful in iterative design practice.

CAVITATION PHYSICAL DESCRIPTION

Here we provide a brief overview of the physical underpinnings of cavitation specifically to elucidate understanding of the simplified 1D models and subsequent discussion on deriving the cavitation characteristic with CFD tools. AxSTREAM® provides an NPSHr prediction and is semi-empirical in nature. CFD uses first-principles physics and semi-empirical models (turbulence and RANS) to solve for fluid thermodynamic (pressure, etc.) and kinematic (velocity vector) fields. These fields represent physical quantities. NPSH can be related to physical quantities. It bears restating that in both the 1D methods and CFD study (and physical reality) cavitation is associated with the pressure field in the flow, regardless whether we have detailed (CFD) or coarse (1D) resolution of this field. Understanding how to associate known parameters of the flow to the pressure field will therefore be a critically useful tool.

NPSH has the following definition:

$$NPSH := \frac{P_t - P_{vap}}{\rho g} = \frac{P_s}{\rho g} + \frac{c^2}{2g} - \frac{P_{vap}}{\rho g} \tag{3}$$

We often encounter different versions of NPSH, and they can be massaged into the above forms (they are equivalent).

$P_t = total\ pressure$
$\rho = fluid\ density$
$g = gravitational\ constant$
$P_s = static\ pressure$
$c = local\ velocity$
$P_{vap} = fluid\ saturation\ pressure\ at\ inlet\ temperature$

We have several "NPSH" values to keep track of. NPSHa is the available head at the inlet of the pump, given by the formula above. It stays constant for a particular operating condition because it is defined by the fluid inlet pressure and temperature as seen from the above formula. NPSHr is the REQUIRED head necessary to either prevent cavitation, or, if not to prevent phenomenological cavitation, to avoid its effects such as damage or performance loss associated with certain severity of the cavitation. What is cavitation? It is the brief vaporization and bubble collapse at surfaces of the blades and endwalls. How does this happen? Clearly, the local fluid static pressure has to drop below its saturation pressure at some location at the local temperature. Therefore, we can define a criterion for local bubble formation as:

$$P_s(local) = P_{vap}(@local\ temperature) \tag{4}$$

This of course is a slight approximation, as there are transient effects involved including the possibility of dipping below the vapor pressure yet not having nucleating agents (preventing bubble nucleation) as well as consideration of the time it takes to form the bubble (if the location of pressure dip is relatively small and velocity passes the fluid volume through in shorter than the nucleation time, the cavitation is mitigated). We are ignoring these effects for this analysis.

So, what then causes the local static pressure to drop below the vapor pressure? The answer is local acceleration of the fluid since total pressure in the relative frame is preserved. Therefore, we can reformulate the simple criteria for bubble formation as:

$$P_t - \frac{1}{2}\rho c^2 = P_{vap} \tag{5}$$

We can divide through to convert to the head metric that many industrial pump practitioners prefer:

$$\frac{P_t}{\rho g} - \frac{c^2}{2g} = \frac{P_{vap}}{\rho g} \tag{6}$$

One should observe that if we rearrange the terms, we have the following condition for cavitation to occur in the "steady-state" sense approximation:

$$\frac{P_t - P_{vap}}{\rho g} = \frac{c^2}{2g} \tag{7}$$

$$NPSHa = \frac{c^2}{2g}\ [local\ cavitation\ condition] \tag{8}$$

We can formulate a parameter called NPSHr, or the required suction head to prevent the above condition as:

$$NPSHr := \frac{c_{max}^2}{2g} \tag{9}$$

$$c'_{max} = maximum\ velocity\ in\ the\ flow\ field \tag{10}$$

It should be noted that the value and actual location of the maximum velocity is difficult to predict. It most often occurs on the tip suction side surface of the impeller blade near the leading edge. However, in order to fully understand the onset of cavitation, detailed CFD simulation or experimental data is necessary. Let's examine the above definition for consistency with the empirical equations. It is common to define a parameter called cavitation suction lift as the difference between the available suction head and required suction head, so that a positive value indicates satisfactory absence of cavitation while negative values indicate cavitation occurring (evaluated either analytically via simulation or experimentally by observing drop in head).

$$H_{cs} = NPSHa - NPSHr \tag{11}$$

$$H_{cs} = \frac{P_t - P_{vap}}{\rho g} - \frac{c_{max}^2}{2g} \tag{12}$$

It can be observed, that if the cavitation suction lift is set to zero, where in the simple steady model it would be predicted that cavitation would start occurring, we have the following condition:

$$H_{cs} = 0 = \frac{P_t - P_{vap}}{\rho g} - \frac{c_{max}^2}{2g} \tag{13}$$

$$\frac{P_t - P_{vap}}{\rho g} = \frac{c_{max}^2}{2g} \tag{14}$$

This is the same as the previously derived steady state condition, so the analytical definition of NPSHr is consistent. In practice, interaction of the fluid with moving walls means that taking the static pressure field and the velocity field will likely result in slightly different effects when evaluating simulation results because the assumption of conservation of total pressure is not truly accurate. Therefore, in addition to relating NPSHr to the velocity field, we can relate it to the pressure field to obtain another validation method. The condition of steady-state cavitation occurs when:

$$P_s(local) = P_{vap}(@local\ temperature) \tag{15}$$

Let us then convert the cavitation suction head into a pressure parameter by multiplying through:

$$\rho g H_{cs} = \rho g(NPSHa - NPSHr) = P_t - P_{vap} - \frac{1}{2}\rho c_{max}^2 = P_{s,min} - P_{vap} \tag{16}$$

Thus, we can rewrite:

$$P_{s,min} = P_t - \rho g(NPSHr) \tag{17}$$

$$\rho g(NPSHr) = P_t - P_{s,min} \tag{18}$$

So now we have several ways to compare semi-empirical cavitation predictions (like those in AxSTREAM®) with the first-principles derived RANS steady-state CFD results:

Method 1: Convert NPSHr prediction to equivalent velocity and pressure conditions (convert 1D prediction to fluid physical parameter)

Step 1: convert 1D NPSHr predicted value to velocity and pressure fields according to

$$2g\ NPSHr\ = c_{max}^2 \tag{19}$$

$$P_{s,min} = P_t - \rho g(NPSHr) \tag{20}$$

Where the total pressure is taken as the inlet total pressure.
Step 2: Graphically or analytically extract the velocity field and static pressure field (iso-surfaces)
Step 3: compare the minimal value of static pressure [should be near blade surface]
Step 4: compare maximum value of velocity
Step 5: examine iso-surfaces for further analysis

Method 2: Convert CFD field results to equivalent NPSHr values (convert fluid physical parameters to equivalent NPSHr)

Step 1: Post process CFD results to obtain velocity fields and static pressure fields in domain
Step 2: Also graphically plot isosurfaces of fields for later analysis
Step 3: Extract maximum velocity in applicable domain

Step 4: Extract minimum static pressure in applicable domain
Step 5: Convert to NPSHr based on velocity:

$$NPSHr := \frac{c_{max}^2}{2g} \tag{21}$$

Step 6: Convert to NPSHr based on pressure:

$$NPSHr = \frac{P_t - P_{s,\min}}{\rho g} \tag{22}$$

Step 7: Examine iso-surfaces for further analysis

Of course, 2-phase transient VOF methods will be more accurate than steady-state 2-phase VOF simulations because the process of bubble nucleation, growth, and collapse is fundamentally transient and turbulent. However, we will also show that steady-state 2-phase VOF with the Schnerr-Sauer cavitation model, a simplification of the Rayleigh-Plesset cavitation model that neglects the effects in bubble growth due to viscosity and surface tension, does a reasonably good job predicting cavitation and NPSHr when compared to 1D predictions that are further tuned to extensive test data. Furthermore, the 2-phase methods are more inclusive of true physical phenomenon than performing RANS CFD using a single phase incompressible fluid assumption. However, even the latter is able to provide some valuable information via scrutiny of the pressure and velocity field using the above methods to check whether the local pressure falls below the vapor pressure.

MODELING AND PREDICTION

Basis Of 1D Methods

Here we partially derive and describe the method for 1D prediction of NPSHr in a pumps used in AxSTREAM®. This method is based on the description of Lomakin (1966). A simple, purely radial 1-dimensional machine geometry is used to make the derivation of the important relationships possible. Also, it is assumed that the flow follows the shape of the blade. Therefore, off-design non-zero incidence conditions are not applicable to this analysis, and the resulting model will only be valid for the zero-incidence condition. Furthermore, we start the analysis with the assumption of purely meridional inflow, and then extend the method to general swirling flow. The analysis starts with balancing the force-momentum equation in the tangential direction for an ideal purely radial pump inlet:

$$dr \cdot db \cdot \Delta p \cdot Z \cdot r = k_1 \cdot \rho \cdot 2\pi r \cdot db \cdot V_m \frac{\partial (V_u r)}{\partial r} dr \tag{23}$$

Where dr and db are infinitesimal lengths of a fluid volume in the radial and axial directions, respectively, Z is the number of blades. The constant k_1 is related to the flow contraction due to blade thickness, while V_m and V_u are the meridional and tangential (circumferential) velocity components. Simplifying and rewriting the previous equation yields

$$\frac{\Delta p}{\rho} = k_1 \cdot \frac{2\pi}{Z} V_m \frac{\partial (V_u r)}{\partial r} \tag{24}$$

It is necessary to make a simplifying assumption that the blade inlet angle is near constant in the streamwise direction (which is the radial plane because the analysis assumes a simple purely radial pump) at the leading edge, leading to the convenient substitution:

$$\frac{\partial (V_u r)}{\partial r} = 2U_1 \tag{25}$$

So that the partial derivative can become an algebraic expression shown in Equation (25). The above simplification is only necessary to make at the leading edge, which is why in Equation (25) the substitution is specifically at U_1, indicating at the leading edge, and presently not distinguishing between hub and tip per our 1-dimensional analysis.

$$\frac{\Delta p}{\rho} = k_1 \cdot \frac{4\pi}{Z} V_{m1} U_1 \tag{26}$$

Inserting the energy equation in the relative reference frame on the pressure and suction sides of the blade,

$$\frac{\Delta p}{\rho} = \frac{W_{max}^2 - W_{min}^2}{2} = \frac{(W_{max} + W_{min})\Delta W}{2} = W \cdot \Delta W \tag{27}$$

Kinematic relations of a blade cascade also establish the following relation. It is important to emphasize that, as stated at the start of the analysis, there is no distinction between the flow angle and metal angle. Therefore, the analysis applies most directly to zero-incidence conditions. The intent of the angles in Equation (28) and further is the blade metal angle, which can be directly extracted from knowledge of the geometry.

$$\frac{\Delta W}{W} = 2k_1 \cdot \frac{\pi}{Z} sin2\beta_1 \tag{28}$$

Also, the maximum velocity at the inlet of the blade can be written as Equation (29).

$$W_{max} = W_1 + \frac{\Delta W}{2} = W_1\left(1 + \frac{k_1\pi}{Z} sin2\beta_1\right) \quad (29)$$

Substituting

$$\Delta H_{in\,max} = \frac{C_{max}^2}{2g} = \frac{W_{max}^2 - U_1^2}{2g} \quad (30)$$

Finally, rewriting,

$$\Delta H_{in\,max} = \frac{U_1^2}{2g}\left[\frac{1}{\cos^2\beta_1}\left(1 + \frac{k_1\pi}{Z} sin2\beta_1\right)^2 - 1\right] \quad (31)$$

This is the derivation of the form of the NPSHr equation based on simplified physical arguments. However, it used many one-dimensional and steady-state simplifications. Real world machines operate in the 3D world with full temporal physics. Therefore, an empirical factor is used to match test data to the functional form derived. This is called C_1.

$$C_1 = \frac{NPSHR}{\Delta H_{in\,max}} \quad (32)$$

So that the equation that predicts the required net positive suction head is given by Equation (33).

$$NPSHR = C_1 \frac{U_{1t}^2}{2g}\left[\frac{1}{cos^2\beta_{1t}}\left(1 + \frac{k_1\pi}{Z} sin2\beta_{1t}\right)^2 - 1\right] \quad (33)$$

It is reasonable and expected at this point that the reader should ask what is meant by NPSHR in this context. After all, the "R" stands for required and the question can be, "required for what?" The answer to this question directly relates to the determination of C_1. While Equation (31) is the derivation for the head or pressure depression reaching inception criteria in a physically ideal case, Equations (32-33) relate to some data-driven correlation. Therefore, the constant can be tuned, at least theoretically, to provide NPSHR to avoid inception, or to estimate 3% TDH drop, or perhaps another criteria. The 3% TDH drop (NPSH3) is realistically what the literature values are derived to determine, and it is the standard to which our 1D code attempts to estimate. It should be noted that Lomakin (1966) suggests that C_1 should be 0.45 for axial-radial impellers and 0.75 for 2D, or fully radial impellers. It is important to notice that in Equation (33) that (i) the NPSHR is dependent on operating conditions and geometry and (ii) that the geometry dependence is most critical at the inlet tip, where relative velocities tend to peak.

Here we now extend the original formula of Equation (33) to apply to swirling flow, wherein the inflow does not necessarily have to be meridional as it enters the leading edge of the impeller. To do so, it is necessary to perform three modifications. The first modification relates the modification of Equation (28) to account for swirl. In deriving Equation (28), Equations (26) and (27) were combined and manipulated, which resulted in the term $\frac{U_1}{W_1}$ to appear because one must divide by W_1^2 to get to Equation (28). The full expression is

$$\frac{U_1}{W_1} = \frac{W_{1U} + c_{1u}}{W_1} = \cos\beta_1 + \frac{c_{1u}}{W_1},\ (C_{1U} \neq 0). \quad (34)$$

It can be substituted as before using the full expression. This is shown in Equation (35).

$$\frac{\Delta W}{W} = 4k_1 \cdot \frac{\pi}{z} \cdot \frac{V_{m1}}{W_1} \cdot \frac{U_1}{W_1} = 2k_1 \cdot \frac{\pi}{z} \cdot 2sin\beta_1 \cdot \left(\cos\beta_1 + \frac{c_{1u}}{W_1}\right) = 2k_1 \cdot \frac{\pi}{z}\left(sin2\beta_1 + 2\frac{c_{1u}}{W_1} sin\beta_1\right) \quad (35)$$

One can easily see that by substituting $c_{1u} = 0$ (strictly meridional inflow) into Equation (35), the original form of Equation 28 is obtained. Confusion should be avoided by noting that the variable c_{1u} uses lower case, which therefore represents, as is standard, the absolute inlet tangential velocity component, rather than the correction factor discussed in Equation (32).

The second modification relates to the trigonometric denominator in Equation (30). During the derivation, again a term of $\left(\frac{W_1}{U_1}\right)^2$ appeared while compiling Equations (29) and (30). This term became $1/\cos^2\beta_1$ when strictly meridional inflow could be assumed, but now becomes a bit more complex, as follows.

$$\frac{W_1}{U_1} = \frac{W_1}{W_{1u} + c_{1u}} = \frac{1}{\frac{W_{1u}}{W_1} + \frac{c_{1u}}{W_1}} = \frac{1}{\cos\beta_1 + \frac{c_{1u}}{W_1}} \quad (36)$$

The third modification relates to the form of Equation (30) when some pre-swirling flow can be present. The velocity triangle needs to be consulted again. When carefully analyzed, the form of the expression takes on Equation (37).

$$\Delta H_{in\,max} = \frac{c_{max}^2}{2g} = \frac{W_{max}^2 - (U_1 - c_{1u})^2 + c_{1u}^2}{2g} = \frac{W_{max}^2 - U_1^2 + U_1 c_{1u}}{2g} \quad (37)$$

When the three corrections shown in Equations (35-37) are applied to Equation (33), we obtain an expression for NPSHR that takes into account the possibility of inflow with a swirl component.

$$NPSHR = C_1\left\{\frac{U_{1t}^2}{2g}\left[\frac{1}{(cos\beta_{1t}+c_{1u}/W_1)^2}\left(1+\frac{k_1\pi}{Z}\left(sin2\beta_{1t}+2\frac{c_{1u}}{W_1}sin\beta_{1t}\right)\right)^2-1\right]+\frac{U_{1t}c_{1u}}{g}\right\} \quad (38)$$

Equation (38) represents the 1D NPSHR correlation for general flow at zero incidence. One can quickly check that Equation (38) reduces to Equation (33) when there is no preswirl at the inlet, which occurs if and only if the tangential velocity component (c_{1u}) is set to zero. It is known that the cavitation and NPSHR value also depends on the fluid motion, particularly variation in flow rate in addition to simply the impeller rotation. It will be noted that the only dependence on operating condition in Equations (33) is the blade tip velocity. In Equation (38), there are further fluid velocity terms, but in the derivation it was assumed that the flow follows the blade perfectly and therefore that incidence is zero. An attempt to include the effects of variable flow rate must also be made and is very useful for predicting the NPSHR profile of a candidate pump in the early design phase. After extensive empirical correlations, it was found that the pressure loss parameter related to incidence loss is the proper choice of correlation. The non-dimensional loss parameter for incidence used in AxSTREAM's 1D code is proportional to the factor shown in Equation (39).

$$\omega_{inc} = \left(\frac{\sin i}{sin\beta_1}\right)^2 \quad (39)$$

where i - incidence angle, β_1 - blade angle, and ω_{inc} is the non-dimensional pressure loss coefficient related to non-zero incidence at the blade leading edge. Equation (40) below converts the loss parameter to units of head increase, also using an empirical factor.

$$NPSHR_{inc} = C_{inc}\left(\frac{sini}{sin\beta_1}W_{1t}\right)^2/2g \quad (40)$$

Where C_{inc} is the empirical tuning factor for incidence. The NPSHR contributions from Equations (38) and (40) are summed together for an overall predicted estimate of NPSHR. Real geometry and test data were used to tune this parameter to the model. The information is proprietary, so only normalized relative and normalized data can be shown. Figure 2 displays the correlation. As can be seen, a proper choice of the tuning parameter shows excellent agreement between test data and predicted NPSHR. The range of the tuning parameter is expected to be in the interval [0, 1]. A different design will be shown in the results section that will show the method and correlation parameter can predict off-design NPSHR reasonably well, especially in the context of design work, where predictions that can be made in a few seconds of computing, in spite of a small trade-off in accuracy, produce significant benefit over even the fastest steady-state CFD methodology which takes hours.

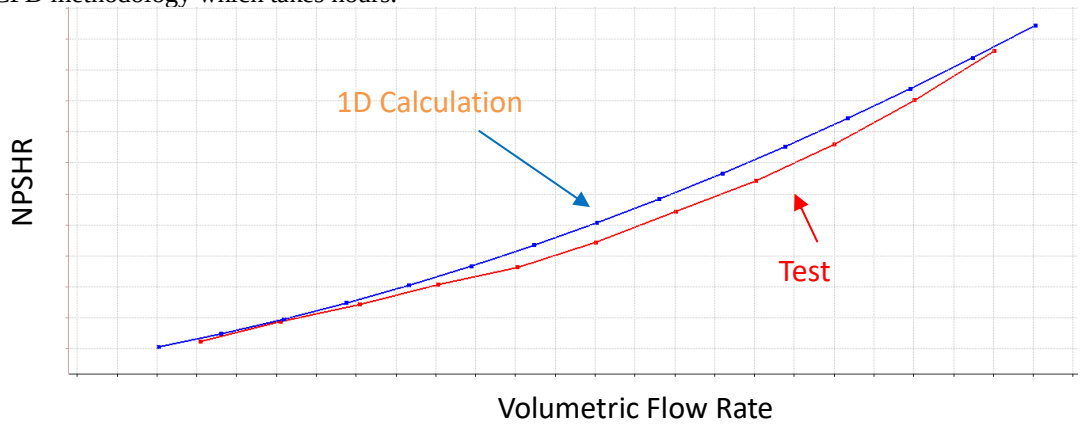

Figure 2 - Tuning of the correlation between incidence and effect on NPSHR

RANS Steady State CFD Methods

To check the 1D semi-empirical methods against more first-principles physics methods, CFD is employed. Of course, CFD as it is applied in industrial situations is itself semiempirical, specifically with the application of RANS turbulence models to properly model flow physics. However, it is recognized as the next best method to gain detailed flow information, next to making detailed measurements of a physical machine. In design work, a physical machine is never available for testing, so CFD is at present the best possible method.

Furthermore, instead of performing transient analyses, we propose steady-state simulations are sufficiently resolving of the important physical phenomena. Critically important is that steady-state simulations are at least an order magnitude less time and computationally expensive. Fundamentally, the CFD code solves numerically the discretized Navier-Stokes' momentum, continuity, and energy conservation equations, which are shown in Equations (41-43).

$$\boldsymbol{u}\cdot\boldsymbol{\nabla}(\rho\boldsymbol{u}) = -\boldsymbol{\nabla}p + \nabla^2((\mu+\mu_t)\boldsymbol{u}) + S_r \quad (41)$$

$$\boldsymbol{\nabla} \cdot (\rho \boldsymbol{u}) = 0 \tag{42}$$

$$\boldsymbol{u} \cdot \boldsymbol{\nabla}(\rho c_p T) = \nabla^2 (k + k_t) T \tag{43}$$

Where S_r is a momentum source term used in this context for modeling rotating domains in turbomachinery. μ_t and k_t are turbulence viscosity and thermal conductivity, which arise in the context of the turbulence models. While we do not discuss turbulence models here explicitly, many excellent references such as Tucker (2016) and Menter (1994) are available. In our work, the k-ε and SST models were used, with consistent results. Both models have been shown to provide reasonably accurate results for a number of industrial internal flow situations. These equations as written here are for an entire sum continuum material. When multiple phases are simulated, as we do in this work, a volume of fluid (VOF) approach is used, where each discretized volume tracks the relative portion of liquid and vapor phases and interphase mass transfer. Thus the equations are modified with source terms for each of the two phases that govern mass transfer between the liquid and vapor phases. The source terms are governed by a model. In the present research, a cavitation model is appropriate and model used is the Rayleigh-Plesset model. The equation that defines this model is given in Equation (44).

$$\frac{p_{sat} - p}{\rho_l} = \left(\frac{3}{2}\right)\left(\frac{dR_B}{dt}\right)^2 + R_B \frac{d^2 R_B}{dt^2} + \frac{2\sigma}{\rho_l R_B} + \frac{4\mu_l}{\rho_l R_B}\frac{dR_B}{dt} \tag{44}$$

Where σ is the surface tension of the fluid and R_B is the radius of a bubble. The reader is referred to the literature for the full derivation of the Rayleigh-Plesset equation, such as Brennen (1995). The important point here is that the rate of change in a typical bubble radius is governed by the fluid properties and the thermodynamic field parameters, specifically pressure and temperate via the saturation pressure, that are determined throughout the flow field solution of the CFD simulation. The bubble radius, in turn, can be directly related to the volume and mass transfer in a discretized fluid element.

For many situations, it is reasonable to ignore all but the first term (corresponding to the growth acceleration, a second order effect, surface tension, and viscous effect) on the right-hand side of Equation (44). This is the Schnerr-Sauer model, and it is the one we use. The modeling equation therefore reduces to Equation (45).

$$\left(\frac{dR_B}{dt}\right)^2 = \frac{2}{3}\frac{p_{sat} - p}{\rho_l} \tag{45}$$

Some additional constants that must be supplied relate to the density of nucleation sites per fluid volume, nucleation site radius, and empirical factors for vaporization and condensation. All parameters were set to their recommended or default values, and the details are described in each code's documentation. It should be emphasized that while it is well understood that the fundamental physics of cavitation is transient, the same may be said of the flow field as well. The steady state approximation aims to extract the relevant quantities of interest by averaging out the transient phenomenon in a numerical fashion (contrasting with fully simulating the transient behavior and physically averaging the parameters of interest). As seen from Equation (45), the rate of bubble volume change is related directly to the pressure field. Thus the steady-state solution predicts the volume fraction of liquid and vapor in the domain and the resulting integral parameters of interest, particular Total Discharge Head (TDH).

RESULTS AND DISCUSSIONS

The subject of the analysis is a centrifugal pump that exists as a conceptual model developed in the AxSTREAM® package and whose fluid volume was exported for CFD analyses. It has an impeller tip diameter of 33cm. This model is based on a known machine whose performance was validated, with scaling and modifications applied for a different duty profile. Therefore, although no direct experimental data is provided for the given model, the design details and are open to disclose. Figure 3 shows the view of the machine.

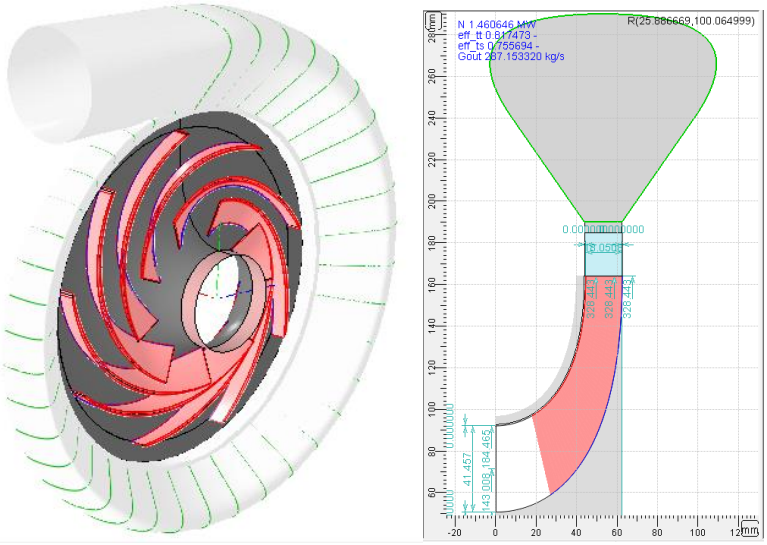

Figure 3 - 3D view (left) and meridional view (right) of subject pump

Table 1 provides the main geometrical properties of the subject pump as an output table from the AxSTREAM code.

Table 1 - Subject pump geometry important parameters

Parameter	Description	Rotor Meridional	Blade	Hub	Mean	Shroud
Prof_angOffLE, deg	LE Theta offset			0	0	0
Prof_angOffTE, deg	TE Theta offset			-107.438	-107.438	-107.438
Cas_K1	LE blade angle (tang)			31.37305	23.6323	14.93
Cas_K2	TE blade angle (tang)			21.27871	21.27882	21.27939
Blade_l1, mm	LE blade height		39.09729			
Blade_l2, mm	TE blade height		18.05085			
FComp_D1t, mm	LE tip diameter	184.4648				
FComp_D1h, mm	LE hub diameter	101.5508				
FComp_D2m, mm	TE diameter	328.4431				
FComp_B, mm	Axial Length	62.4042				

Table 2 provides the rated operating point conditions and design basis for the subject pump of this analysis.

Table 2: Operating characteristics of subject pump

Total temperature at inlet	35 C
Total pressure at inlet	900 kPa
Mass flow rate at inlet	287 kg/s
Shaft speed	6000 rpm
Total-total head	423.87 m
NPSH3	41.95 m
NPSHA	91.38 m
Saturated vapor pressure	5.6267 kPa

The pump was extensively analyzed using both the 1D reduced order model solver in AxSTREAM® and validated by the commercial CFD codes ANSYS CFX and STAR-CCM+. Even though test data was not explicitly available for this configuration, the use of independent CFD codes that each used different mesh settings and solvers and that agreed well with each other and the test data provide confidence that the methodology is sound and accurate.

Two sets of simulations were performed. The first set provided performance curve information. The simulations were performed by

setting the outlet boundary condition to specified mass flow rate, with a specified total inlet pressure at the inlet. A single passage blade row was simulated with a mixing plane interface between the rotor and diffuser and volute domains with an appropriate pitch change. Rotationally periodic and smooth wall conditions were applied as appropriate for the symmetry and wall surfaces, which included the blade, hub, and shroud. These simulations were performed over a range of flow rates and for three operating speeds. The results are displayed in Figure 4. The results showed very close agreement with each other, providing confidence in the methods.

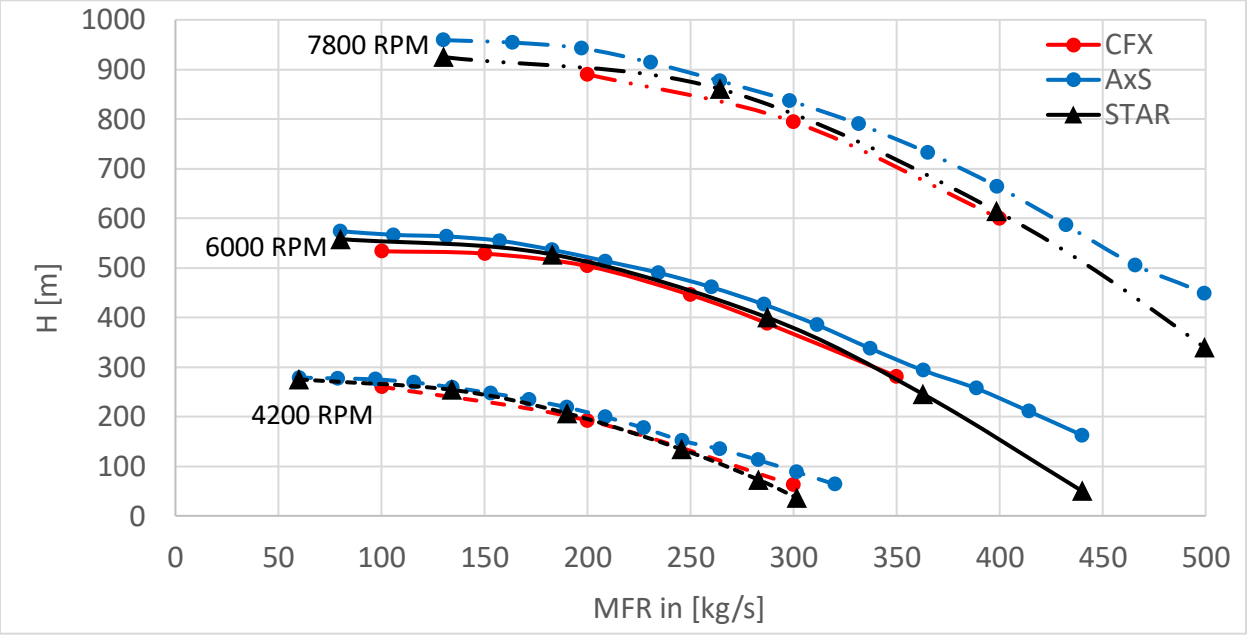

Figure 4 - Pump performance curves predicted by 1D code and independent commercial CFD packages. All predictions show excellent agreement.

The second set of simulations that were performed were done to obtain cavitation characteristic curves. These simulations involved only a single blade passage as the domain and the volute was not simulated because it is not expected in most situations to observe cavitation effects from the volute domain. Therefore, the head does not correspond directly to the performance curves because the losses through the volute are not considered. The method to evaluate cavitation is to use each operating point by setting speed and mass flow, and adjust the inlet total pressure for each simulation. Adjusting the inlet total pressure effectively adjust the net positive suction head provided to the inlet of the simulated pump. The main output of the cavitation simulation is the outlet pressure, which effectively allows computation of the integral parameter of total discharge head for the pump impeller. The physics, as previously described, was modelled in steady state using the Schnerr-Sauer cavitation model and a VOF approach with homogenous model (thermodynamic and momentum properties for the two phases are equal in each fluid volume of the computational grid).

Effectively, this method is very similar to the methodology of establishing a cavitation characteristic in a physical experiment, whereby a physical pump would be subjected to varying inlet pressure conditions and the TDH would be measured as a resulting parameter. It is clear that this is a fairly computationally involved process even though only steady-state simulations are performed because for each operating conditions on the performance curve an entire set of simulations must be run. For this reason we chose three operating conditions on the design speedline corresponding to the rated condition and two lower flow rates.

In order to have confidence in the accuracy and consistency of our CFD method, we conducted a mesh sensitivity and turbulence model sensitivity study using the ANSYS CFX solver. The results, shown in Figure 5, reveal baseline TDH agreement within 3% for all the methods and supercavitation breakdown within a very close range. Here again, confidence in the method was lifted. We then performed the analysis for the design point (287 kg/s), 200kg/s, and 100kg/s flow rates. The analysis was performed using both STAR-CCM+ and CFX codes to provide further confidence that the method is relatively universal in the sense of producing consistent results as long as proper convergence and simulation setup was monitored. The results are shown in Figure 6 through Figure 8.

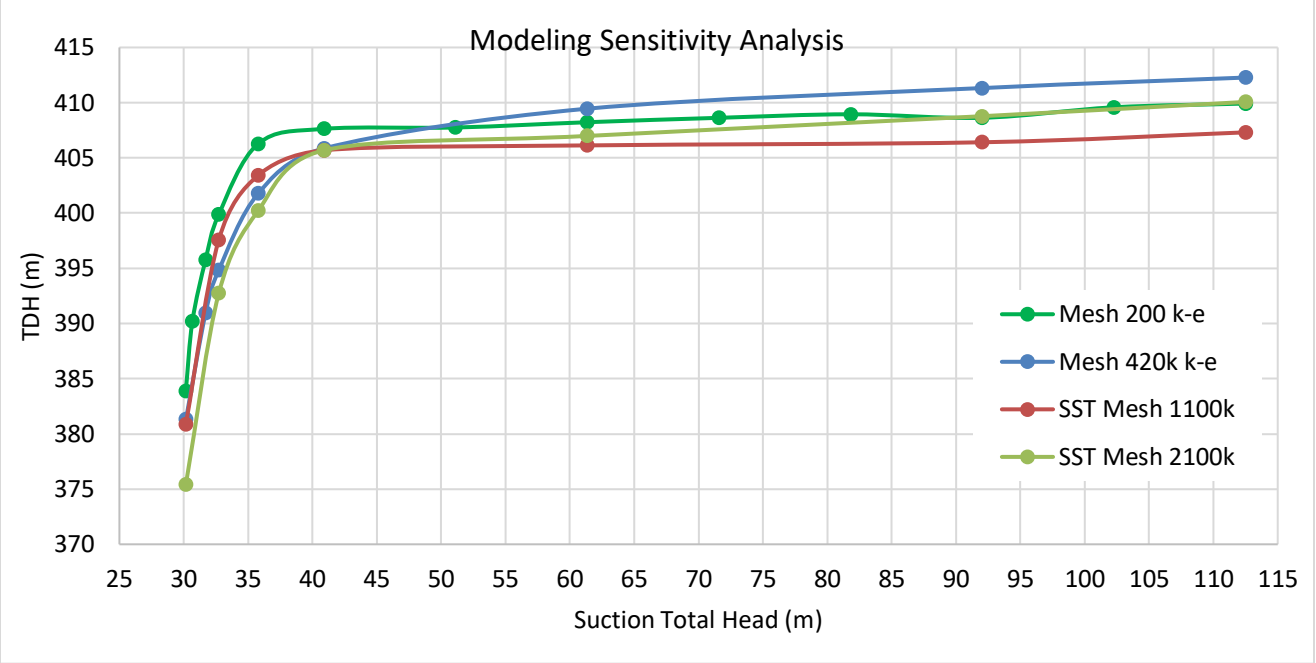

Figure 5 - Modeling sensitivity study results for cavitation characteristic showing the effect of variable computational grid densities and turbulence models at rated conditions (6000RPM, 287kg/s MFR)

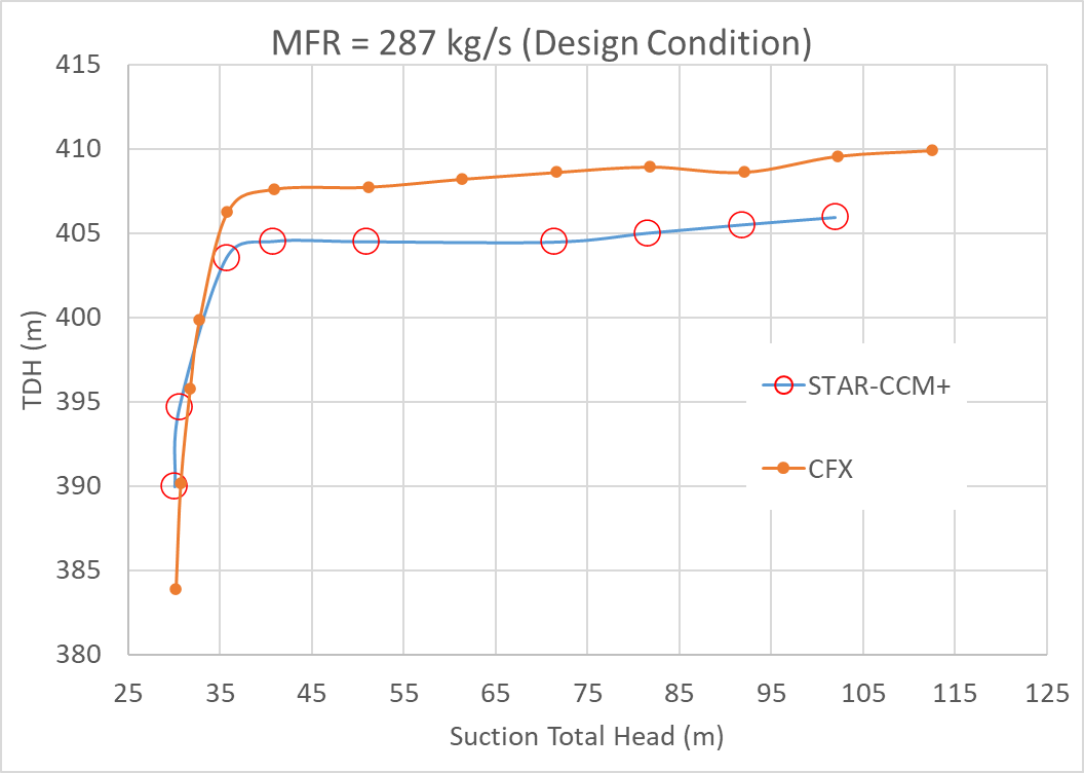

Figure 6 - CFD predicted cavitation characteristic for design operating point

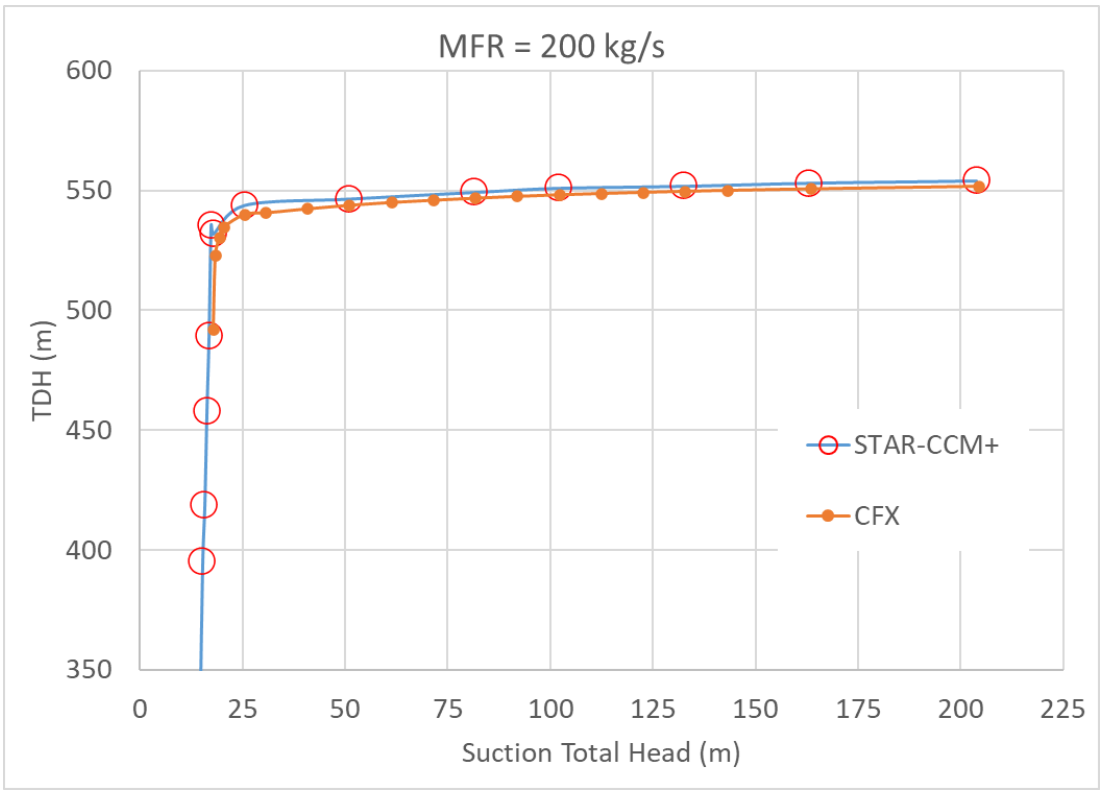

Figure 7 - CFD predicted cavitation characteristic for flow rate lowered to 200kg/s

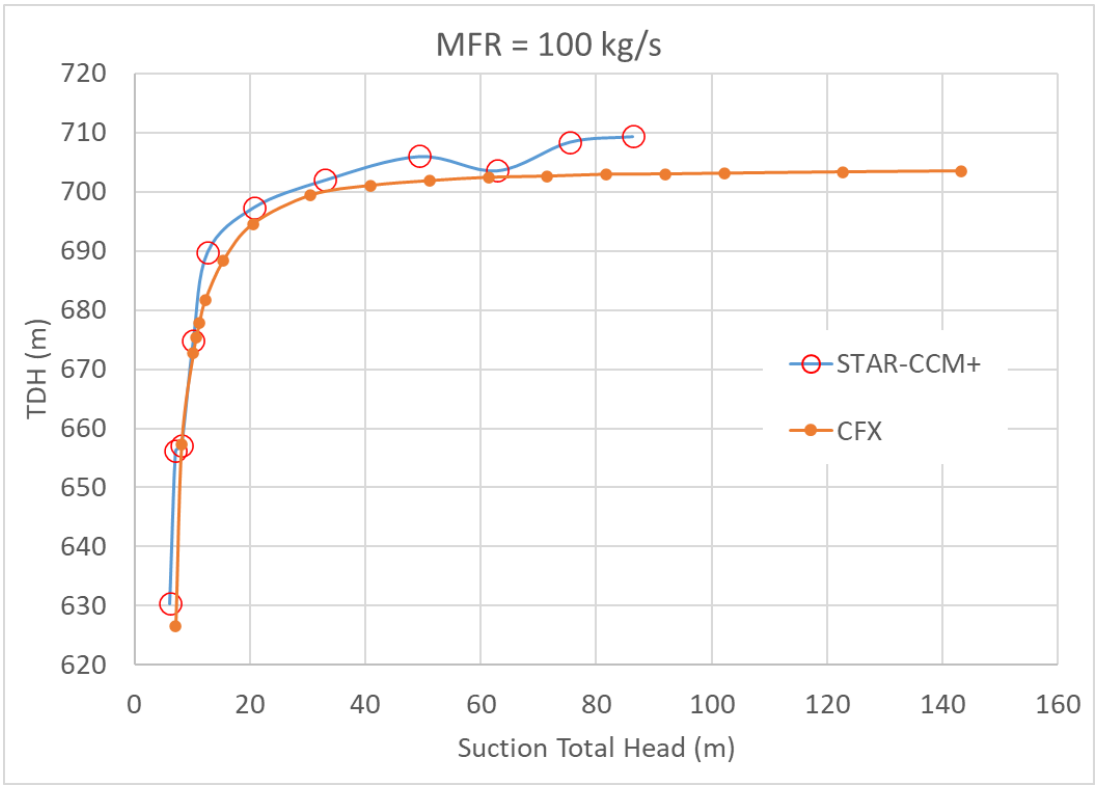

Figure 8 - CFD predicted cavitation characteristic for flow rate lowered to 100kg/s

It is also possible to scrutinize the flow field to check details about the flow, and particularly of interest in this study, the progression of cavitation phenomenon at various suction head conditions. As emphasized particularly before, the 1D code is not able to, fundamentally, say anything about cavitation because it does not model any of the true physics of cavitation. It is only able to predict a single value for each operating condition based that geometry and operating condition. Specifically, it provides a value of NPSHR as a condition of

avoiding something, which is a drop in TDH performance. We see this as very valuable information for design work, where results are needed fast for quick iterative design improvements. On the other hand, we must also recognize that this does not come anywhere near to painting the whole picture or satisfying our scientific curiosity about what are the phenomena occurring in the flow path. Figure 9, therefore, shows some interesting views of the simulated cases, specifically plotting isosurfaces of the condition where the local pressure is equal to the saturation pressure of the fluid. Since the TDH head drop off of 3% occurs at 32.7m of inlet head, it is clear that significant cavitation phenomenon is occurring up to perhaps 61m of inlet head which would be considered satisfactory from an NPSHR3 perspective, but there may be damage accumulation due to bubble collapse near impeller surfaces.

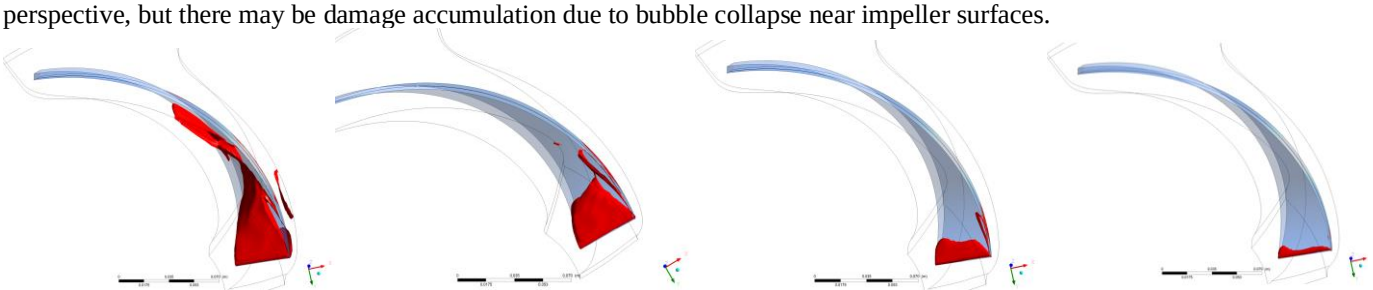

Figure 9 - Isosurfaces of the condition where the local static pressure equals the saturated vapor pressure in the flow field for the design flow rate and progressively decreasing suction head from right (inception) to left (supercavitation). Suction heads correspond to 92m, 61m, 41m, and 32m from right to left at the rated flow rate.

Finally, we are able to directly compare the 1D prediction to the CFD, where the CFD method marks off where each characteristic curve drops off by 3% from the flat TDH baseline value. This is shown in Figure 10. It must be recalled here that the 1D prediction of based on a combination of the zero-incidence, or design, NPSHR empirical method of Lomakin (tuned to a range of pumps) with an incidence correction tuned to a specific test case. The curves trend in a similar fashion, and the constant can be tuned to a specific class of machines when even more accurate agreement is needed. In this case, the 1D prediction is most likely still in the range where cavitation occurs, but slightly conservative related to the NPSHR3 criterion.

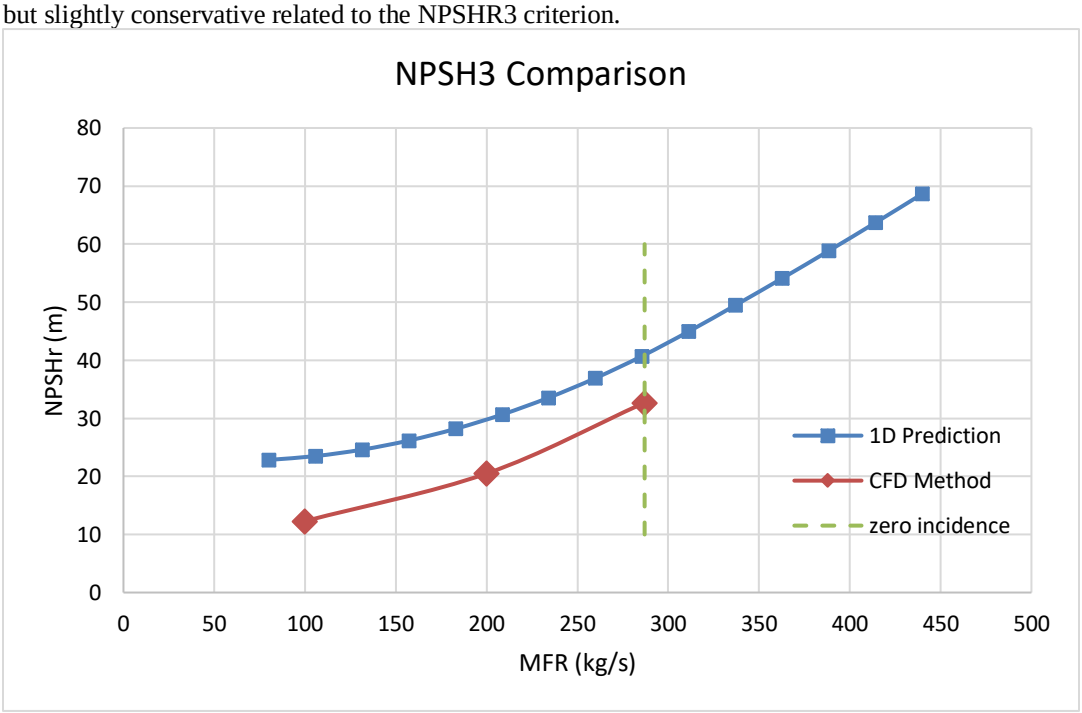

Figure 10 - 1D prediction of NPSHR3 versus the CFD predictions for the design speedline

CONCLUSIONS

It has been shown in this research that Lomakin's method for predicting NPSH3 at design conditions has been extended to the capability to predict varying NPSHr at variable flow rates by using the incidence loss methodology infrastructure which is already built into 1D loss model correlations in AxSTREAM's® hydrodynamic performance prediction code. A single empirical constant seems to provide for ability to empirically tune the incidence correction for NPSHr sufficiently well for a single particular design type, as is evidenced, albeit with a single case, by the good matching of test data to 1D predictions when the incidence model was tuned.

Proven CFD analyses methods employing steady-state RANS with a homogeneous volume of fluid (VOF) method with Schnerr-Sauer cavitation model were used to produce cavitation characteristic curves for a conceptual pump design. Sensitivity analysis of this method

was performed with respect to grid density and turbulence model, as well as grid and solver type, and all results were in good agreement with each other. Other researchers have similarly found this method to be able to reliably predict a cavitation characteristic.

By performing the CFD analysis on the subject conceptual pump we showed that the semi-empirical 1D NPSH3 prediction model performed reasonably well at predicting the trend of the curve as a function of flow rate, even though the model was consistently off by an offset. Further, the 1D model, or more specifically the incidence correlation, was tuned for a different pump, so it is perhaps not surprising that such a simple model would not universally predict the correct value of NPSH3 across all operating conditions. The fact that the trend followed well, and that the deviation was not very large is perhaps indicative that additional sophistication can be added to the incidence correlation (and perhaps also Lomakin's term for zero incidence condition), perhaps through the inclusion of previously uncorrelated geometry parameters, so that the 1D fast nature is maintained with improved predictive capability. This will be the subject of future investigations. We also reinforce the statement that the deviation in NPSH3 prediction is not very large. It was seen in Figure 9 that the cavitation inception occurs that a suction head that is approximately 3 times the suction head at which a 3% drop in TDH occurs (NPSH3). Therefore, the 1D prediction curve of Figure 10 lies well within the zone of cavitation inception and NPSH3, and is a conservative prediction for the particular design case studied here.

FUTURE WORK

We seek ways to further improve the methodology presented here for increased accuracy and wider scope of applicability, as well as to provide additional validation to enhance confidence that the method is sound. The following is in the early stages of investigation, and we hope to report progress in future work.

1. Enhancement of the sophistication of the 1D model to increase accuracy and scope of applicability
2. Validate prediction with real world data of physical pumps
3. Performing fully transient cavitation analysis in CFD

It is important to note that the first above point highly depends on the latter point: the availability of either real world data and/or additional numerical experimentation. Regarding the second point, we have good indication that a limited data set of newly designed pumps will be available for validation. Of course, we continue to seek reliable real-world test data. Finally, with regard to additional numerical experimentation, it is of engineering interest to evaluate the errors or discrepancies between transient and steady methods used here because the fundamental underlying phenomena is transient in nature. Although transient CFD analysis of cavitation is by no means new, as far as we are aware it has not been performed for comparison with and to better inform reduced order 1D models.

NOMENCLATURE

c	=	local fluid velocity	(m/s)
C_1	=	matching factor relativng NPSHR and $\Delta H_{in\ max}$	
C_{inc}	=	empirical tuning factor for incidence losses	
c'_{max}	=	maximum velocity in flow field	(m/s)
CFD	=	computational fluid dynamics	
c_p	=	constant pressure specific heat	(J/kg-K)
db	=	infinitesimal lengths of a fluid volume in axial direction	(m)
dr	=	infinitesimal lengths of a fluid volume in radial direction	(m)
g	=	gravitational constant	(m/s^2)
H_{cs}	=	cavitation suction lift	(m)
$\Delta H_{in\ max}$	=	total suction head drop	(m)
i	=	incidence angle	(deg)
k	=	thermal conductivity	(W/m^2-K)
k_1	=	contraction ratio at inlet due to blade thickness at inlet	
k_t	=	turbulent thermal conductivity	(W/m^2-K)
$NPSH$	=	net positive suction head	(m)
$NPSH_a$	=	available net positive suction head	(m)
$NPSH_r$	=	required head necessary to prevent cavitation or its effects	(m)
$NPSH_3$	=	required inlet head to achieve 3% drop in TDH	(m)
Δp	=	pressure gradient	(Pa)
P_s	=	static pressure	(Pa)
P_{sat}	=	fluid vapor pressure	(Pa)
$P\infty$	=	local liquid static pressure	(Pa)
Pt	=	total pressure	(Pa)
P_{vap}	=	fluid saturation pressure at inlet temperature	(Pa)
$RANS$	=	Reynolds-averaged Navier Stokes	

R_B	=	bubble radius	(m)
S_r	=	momentum source term	(kg-m/s)
T	=	fluid temperature	(K)
TDH	=	total discharge head	(m)
U_1	=	inlet blade tangential velocity	(m/s)
V_m	=	meridional velocity component	(m/s)
V_u	=	tangential (circumferential) velocity component	(m/s)
VOF	=	volume of fluid	
W_{max}	=	maximum relative velocity at blade inlet	(m/s)
W_{min}	=	minimum relative velocity at blade inlet	(m/s)
ΔW	=	maximum and minimum relative velocity difference at inlet	(m/s)
W_1	=	mean relative velocity at blade inlet	(m/s)
Z	=	blade number	

Greek Symbols

β_1	=	inlet relative flow angle or metal angle	(deg)
μ	=	liquid dynamic visocity	(Pa-s)
μ_t	=	turbulence viscosity	(Pa-s)
ρ	=	liquid density	(kg/m^3)
σ	=	surface tension	(N/m)
ω_{inc}	=	incidence loss parameter	

REFERENCES

ANSYS, 2020, ANSYS CFX 2020 R2 CFX-Solver Modelling Guide, Manual, ANSYS, Inc.

Bakir, F., Rey, R., Gerber, A.G., Belamri, T. and Hutchinson, B., 2004. Numerical and experimental investigations of the cavitating behavior of an inducer. International Journal of Rotating Machinery, 10(1), pp.15-25.

Brennen, C.E., 1995. Cavitation and bubble dynamics. Oxford University Press.

Czyszczewski, M.F., 2021. Understanding Net Positive Suction Head Requirements for Pumps. Power, 165(2), pp.26–29.

Li, W.G., 2014. Validating full cavitation model with an experimental centrifugal pump. Task Quarterly, 18(1), pp.81-100.

Lomakin, A.A., 1966. Centrifugal and Axial Pumps [in Russian].

Marini, A., Salvadori, S., Bernardini, C., Insinna, M., Martelli, F., Nicchio, A. and Piva, A., 2011, March. Numerical prediction of cavitation inception in centrifugal impellers. In 9th European Turbomachinery Conference (pp. 21-25).

Mejri, I., Bakir, F., Rey, R. and Belamri, T., 2005, January. Comparison of Computational Results Obtained From a VOF Cavitation Model With Experimental Investigations of Three Inducers: Part I—Experimental Investigations; Part II—Numerical Analysis. In Fluids Engineering Division Summer Meeting (Vol. 41987, pp. 1147-1191).

Menter, F.R., 1994. Two-equation eddy-viscosity turbulence models for engineering applications. *AIAA journal*, *32*(8), pp.1598-1605

Pei, J., Osman, M.K., Wang, W., Appiah, D., Yin, T. and Deng, Q., 2019. A practical method for speeding up the cavitation prediction in an industrial double-suction centrifugal pump. Energies, 12(11), p.2088.

Schiavello, B. and Visser, F.C., 2009. Pump Cavitation: various NPSHR criteria, NPSHA margins, impeller life expectancy. In Proceedings of the 25th international pump users symposium. Texas A&M University. Turbomachinery Laboratories.

Siemens, P., 2018. Simcenter STAR-CCM+ User Guide V16.04. *Plano: Siemens PLM*.

Tucker, P.G., 2016. Advanced computational fluid and aerodynamics (Vol. 54). Cambridge University Press.

ACKNOWLEDGEMENT

The authors wish to thank the management of SoftInWay for their support and permission to publish this material.